J. Membrane Biol. 117, 29–44 (1990)

The Journal of
Membrane Biology

Whole-Cell Currents in Macrophages: I. Human Monocyte-Derived Macrophages

D.J. Nelson, B. Jow, and F. Jow
Departments of Medicine and Neurology, University of Chicago, Chicago, Illinois 60637

Summary. We examined the variability of occurrence and frequency of voltage-dependent whole-cell currents in human peripheral blood monocyte-derived macrophages (HMDM) maintained in culture for up to three weeks. An increase in cell capacitance from an average value of 9 pF on the day of isolation to 117 pF at 14 days accompanied growth and differentiation in culture. The average resting potential was approximately −34 mV for cells beyond two days in culture. Cells exhibited a voltage- and time-dependent outward current upon membrane depolarization above approximately −30 mV, which appeared to be composed of a number of separate currents with variable expression from donor to donor. Three of these currents are carried by K^+. The frequency of each outward current type was calculated for 974 cells obtained from 36 donors. The HMDMs in these studies exhibited two 4-aminopyridine (4-AP) sensitive, time-dependent outward currents (I_A and I_B) that could be differentiated on the basis of the presence or absence of steady-state inactivation in the physiological potential range, time course of inactivation during maintained depolarization, as well as threshold of activation. The 4-AP-insensitive outward current activated at approximately 10 mV. One component of the 4-AP insensitive-outward current (I_C) could be blocked by external TEA and by the exchange of internal Cs^+ or Na^+ for K^+. The probability of observing I_B and I_C appeared to be donor dependent. Following total replacement of internal K^+ with Cs^+, two additional currents could be identified (*i*) a delayed component of outward current (I_D) remained which could be blocked by low concentrations of external Zn^{2+} (4 μM) and was insensitive to anion replacement in the external solution and (*ii*) a Cl^- current with a reversal potential which shifted in the presence of external anion replacement and which was irreversibly inhibited by the stilbene SITS. The activation of a prominent time-independent inward current was often observed with increasing hyperpolarization. This inward current was blocked by external Ba^{2+} and corresponded to the inwardly rectifying K^+ current. Neither inward nor outward current expression appeared dependent on whether cells were differentiated in adherent or suspension culture nor was there demonstrable differential current expression observed upon transition from suspension to adherent form.

Key Words macrophage · K^+ conductance · Cl^- conductance · ion channel · patch clamp · differentiation

Introduction

When monocytes leave the vascular compartment and accumulate within body tissues, they mature and differentiate into macrophages (van Furth et al., 1982). Comparable morphologic, metabolic, and functional changes occur when monocytes are maintained in culture (Bennett & Cohn, 1966; Johnson, Mei & Cohn, Ackerman & Douglas, 1979). In the present studies, we employed in vitro human monocyte-derived macrophages (HMDM) as a model system in which to study the development of ion channel expression accompanying this process.

We characterized five separate outward currents in HMDM. Three of these currents are carried by K^+, a fourth appears to be a nonselective cation current, while the fifth is an anion-selective current. Of the K^+ outward currents, we were able to demonstrate a TEA-sensitive, Ca^{2+}-activated K^+ conductance as well as a rapidly inactivating 4-aminopyridine (4-AP) sensitive outward current both of which had been described previously for HMDMs (Gallin & McKinney, 1988). In addition, we demonstrated for the first time, a time-dependent K^+ current which does not show steady-state inactivation, a nonselective cation current which activates with a delayed time course in the depolarized voltage range, and an outwardly rectifying Cl^- current which is inhibited by the stilbene SITS (4-acetamido-4′isothiocyano-2,2′-stilbene disulfonate). An inwardly rectifying K^+ conductance which has previously been linked to macrophage adherence (Gallin & Sheehy, 1985) was also present.

We were unable to demonstrate any correlation in differential current expression to state of differentiation, mode of differentiation (suspension *versus* adherence), or transition from suspension to adherence culture, although, in general, outward current amplitude for each current type increased with time in adherent culture, as has been observed for peritoneal macrophages (Ypey & Clapham, 1984). Interestingly, the frequency of two of the current types, the time-dependent K^+ current which did not exhibit steady-state inactivation (I_B), and the Ca^{2+}-activated K^+ current (I_C), appeared to be donor dependent.

Materials and Methods

Peripheral Blood Leukocyte Separation

Percoll Gradient Isolation Technique

Peripheral venous blood samples were collected from healthy human volunteers. Mononuclear cells were separated from neutrophils and erythrocytes by Ficoll-Hypaque density gradient centrifugation (Zeller et al., 1986). The mononuclear cell fractions were washed with phosphate-buffered saline solution (PBS) and further purified by using the Percoll (Pharmacia Fine Chemicals, Piscataway, NJ) density gradient centrifugation method described by Wright and Silverstein (1982). The monocyte-rich fractions collected from the upper portion of the Percoll gradient were combined and washed four times with cold PBS. Cell counts were determined by routine hemocytometry. Cell viability, as determined by trypan blue dye exclusion, was routinely greater than 95%. The monocyte-rich fraction consisted of 60–90% monocytes and 10–40% lymphocytes, as determined by latex ingestion, nonspecific esterase, and peroxidase staining.

Human monocyte-enriched leukocyte fractions, suspended in Medium-199 (Gibco Laboratories, Grand Island, NY) containing 10% autologous human serum 100 U/ml penicillin and 50 μg/ml streptomycin (M199-AHS), were cultured in Teflon vials (Savillex, Minnetonka, MN) for up to 12 days at 37°C in a 5% CO_2 in air atmosphere prior to their introduction into adherent culture. Cells were cultured on 35-mm plastic tissue culture dishes (Falcon Labware, Oxnard, CA) at a density of 1×10^6 cells per dish in M199-AHS. Cells were maintained in adherent culture for 1–17 days following suspension culture before the one-time use of a culture dish for an electrophysiological experiment.

Adherence Isolation Technique

Cells were alternatively isolated using an adherence technique following the Ficoll-Hypaque density gradient centrifugation step. Cells isolated from the mononuclear fraction were washed three times with RPMI-1640 growth medium, resuspended in RPMI-1640 supplemented with 10% autologous human serum, and plated at a density of 1×10^6 cells/ml on uncoated 35-mm tissue culture dishes which had been finely scored with a fine wire brush. The scoring of the tissue culture dishes greatly aided growth and long term differentiation in culture. After 1-hr incubation, the adherent cells were washed three times with non-serum containing RPMI-1640. Adherent cells were incubated with serum-containing medium and fed the day following the isolation procedure. Both isolation procedures were performed in the absence of exogenously applied lipopolysaccharide. Contaminant endotoxin levels, which would give rise to a basal level of cellular activation, were not determined. Cells used in the electrophysiological experiments from both the percoll and adherence isolation techniques were determined to be macrophages on the basis of adherence following a vigorous washing step in the 1–2-day-old cells and by size and adherence in the older cell cultures. Monocytes maintained in culture for 1 to 2 days measured approximately 10–15 μM in diameter and, unlike lymphocytes with diameters of 6–8 μm, readily attached to the culture dish. By day 4 in either adherent or suspension culture, cells measured greater than 20 μm in diameter and avidly spread onto the culture dish surface.

Electrophysiology

Whole-cell recordings from HMDM membranes were obtained using the techniques of Hamill et al. (1981). A dish containing cultured cells was placed in a chamber on the movable stage of an inverted microscope equipped with phase-contrast optics. Recording pipettes were formed from soda lime glass (Blue-Dot Hematocrit Glass; Fisher Scientific, Pittsburgh, PA) using a vertical puller in a three-stage process. Pipettes were coated with Sylgard 184 (Dow-Corning, Midland, MI) and fire-polished to a final tip diameter of approximately 0.5 μm just before use. Experiments were performed at room temperature (21–23°C).

Solutions

The standard internal (pipette) solution with 38 nM free Ca^{2+} contained (in mM): 140 KCl, 2 $MgCl_2$, 2 $CaCl_2$, 11 EGTA-KOH, and 10 HEPES; pH 7.2. In some experiments the pipette was perfused with solutions of increasing free-Ca^{2+} concentration. For final free-Ca^{2+} levels of 212 and 477 nM, the $CaCl_2$ concentrations used were 6 and 8 mM, respectively. When Cs^+ or Na^+ was used in the internal solution, some fraction of the total KCl was replaced with an isosmolar amount of the desired salt. The bath solution contained (in mM): 140 NaCl, 5.4 KCl, 2 $CaCl_2$, 1 $MgCl_2$, and 10 HEPES; pH 7.4. Changes in the anion or cation composition of the bathing solution were made by isosmolar replacement of either Na^+ or Cl^-.

DNDS (4,4′-dinitro-2,2′-stilbene disulfonic acid disodium salt) DPC (diphenylamine-2-carboxylate) and anthracene-9-carboxylate were purchased from Pfaltz and Bauer (Waterbury, CT) and SITS (4-acetamido-4′-isothiocyano-2,2′-stilbene disulfonate) from Polysciences (Warrington, PA). TEA and 4-AP were obtained from Sigma (St. Louis, MO).

In some experiments a bath perfusion system was employed which allowed for sequential solution changes. Bath solution changes were made at the rate of 1 cc/min. In those experiments in which the bath solution was changed, the bath ground electrode was connected to the bath solution via an agar/saline bridge in order to prevent electrode offset potentials.

Data Acquisition and Analysis

Whole-cell currents were obtained using a List EPC-7 (List Electronic, Darmstadt, FRG) voltage clamp. In general, voltage pulses of 1.7 sec in duration were delivered once every 40 sec. The interpulse interval was sufficient to allow for recovery from the effect of the preceding pulse. The output of the current-to-voltage converter was filtered through a low-pass filter at 1 kHz. The current signal was sampled at 1 kHz by a 12-bit A/D converter (Data Translation 2818, Marlborough, MA) and written into data files using an IBM-AT. Current decays were analyzed as a sum of exponentials by a Fourier method (Provencher, 1976) that determined the number, amplitudes, and time constants of the components. Summary data are expressed as means ± standard error of the mean with the number of experiments in parentheses.

Results

Variability in Whole-Cell Current Activation

Whole-cell voltage-clamp current records were obtained from HMDM maintained in culture for periods of up to three weeks. During this time monocytes displayed a pleomorphic morphology with sizes ranging from 20 to 120 μm in diameter. Although monocyte differentiation was carried out in both suspension and adherent culture using cells isolated either via Percoll density gradient purification or adherence purification, no difference in morphology over time in culture was observed which could be related to either isolation or differentiation technique. All voltage-clamp experiments were carried out on adherent cells. Those cells which were maintained in suspension culture were allowed to adhere to a plastic culture dish for approximately an hour before the electrophysiological recordings were made.

Cellular input resistance was determined under conditions in which all of the K^+ in the pipette solution had been replaced by Cs^+ which blocked all outward current activation. The average input resistance in the Cs^+ solutions was determined to be 3.77 ± 0.93 GΩ (15) over the voltage range of −50 to −20 mV. It was not uncommon to observe the appearance of single-channel currents on whole-cell current records due to the high input impedance of the cells (*see* Fig. 1*C*). Cell capacitance was calculated (in the absence of ionic current) by integrating the current during a 10- to 20-mV voltage step and subtracting a baseline current established approximately 20 msec after the step. A decrease in cell input resistance and an increase in cell capacitance was observed with time in culture (Table 1), and corresponded to the increase in cell size which accompanied cellular differentiation in culture.

Cultured cells displayed a heterogeneity in current activation in response to hyperpolarizing and depolarizing pulses. Current records, representative of the four predominant current patterns observed in voltage-clamped HMDM in normal bathing solution, are presented in Fig. 1. Peak amplitudes of the voltage-dependent currents obtained from the four cells in Fig. 1*A*–1*D* are plotted against membrane potential below each current record. In general, outward current amplitude for each current type increased with time in adherent culture, as has been observed for peritoneal macrophages (Ypey & Clapham, 1984). The major current types could be distinguished on the basis of their voltage-dependent availability, i.e., steady-state inactivation as well as pharmacological sensitivity.

Table 1. Human monocyte-derived macrophage resting membrane properties

Days	Capacitance (pF)	Input Resistance (GΩ)	Specific Membrane Resistance (kΩ · cm²)
1	8.9 ± 0.8(6)	22.2 ± 0.9(4)	198
3	16.3 ± 2.0(4)	6.9 ± 5.3(4)	113
4	35.0 ± 3.1(3)	5.0 ± 1.8(3)	175
7	65.3 ± 3.8(5)	2.8 ± 0.6(5)	182
9	100.6 ± 21.5(3)	3.4 ± 1.5(3)	342
14	117.3 ± 21.4(4)	1.6 ± 0.4(4)	188

Resting membrane properties were determined for cells as function of days following adherence isolation. Input resistance was determined over the voltage range of −50 to −20 mV with Cs^+ as the internal cation. Capacitance was measured by integrating the current during a 10- to 20-mV voltage step and subtracting a baseline established about 20 msec after the step as determined from a nonlinear fit to the data. Specific membrane resistance was calculated assuming a specific membrane capacitance of 1 μF/cm².

Transient Outward Current (I_A)

This current resembles that previously described in a number of cells of the immune system (*see* review by Gallin & Sheehy, 1988) and, in contrast to data obtained from human peripheral blood T lymphocytes, is the most infrequent of the currents found in human monocytes. As described for T lymphocytes and peritoneal macrophages, I_A activated at potentials positive to −40 mV and inactivated at potentials at which currents could be elicited (*see* Fig. 1). Steady-state inactivation was half-maximal at approximately −44 mV. The inactivation process has been well-characterized for this current in J774 cells, T lymphocytes, and murine peritoneal cells and is described in depth in the following paper (Nelson, Jow & Popovich, 1990) for the HMDM and the human alveolar macrophage.

Residual Inactivating Outward Current (I_B)

A second time-dependent outward current, I_B, could be identified in the HMDMs at a much higher frequency than that of I_A. I_B differed from I_A in that (*i*) I_B activated at potentials more positive than I_A, i.e., positive to −10 mV, (*ii*) I_B current showed no steady-state inactivation over the physiological

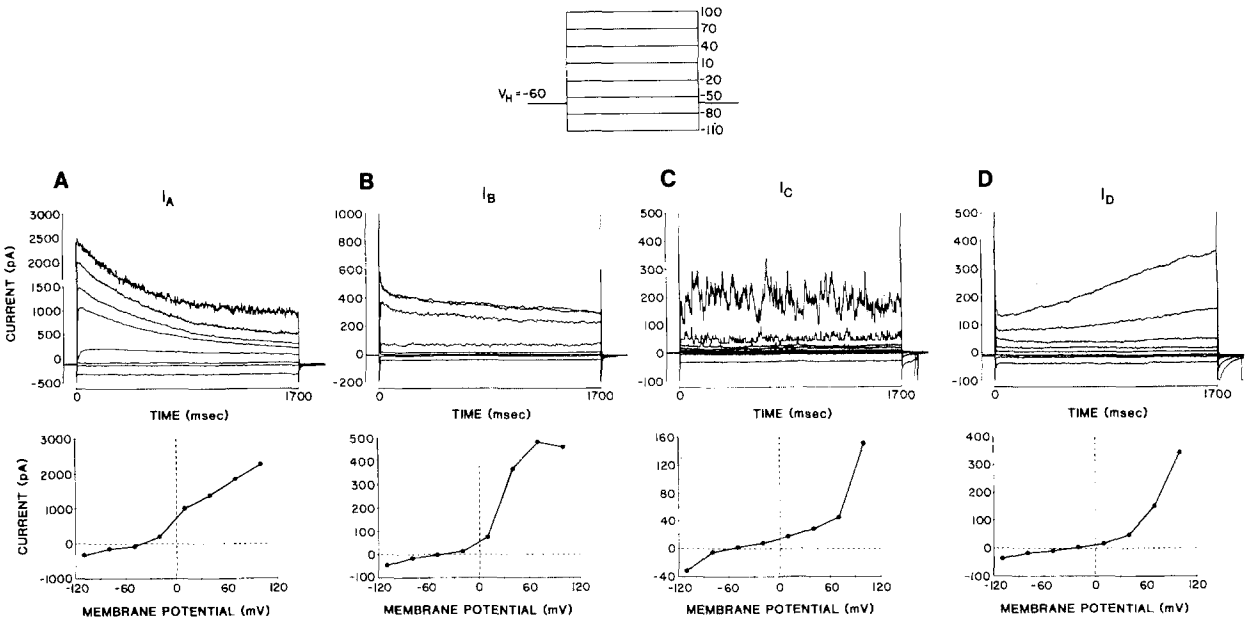

Fig. 1. Representative whole-cell current records demonstrating variability of voltage-dependent outward current in monocyte-derived macrophages. (*A*) Current record from a cell which was maintained for eight days in suspension after isolation and then plated for 12 days before the electrophysiological experiment was performed. (*B*) Current record from a cell six days after isolation and plating. (*C*) Current record from a cell six days after isolation and plating. (*D*) Current record from a cell eight days after isolation and plating. Cells in the four experiments were derived from separate isolations. In all current records, hyperpolarizing and depolarizing pulses 1.7 sec in duration were applied at 40-sec intervals from a holding potential of −60 mV according to the schematized pulse protocol. Unless stated otherwise, all current records in subsequent figures were obtained using the identical voltage pulse protocol. Peak current-voltage relationship is depicted for each of the representative current records. Peak currents for I_A and I_B were measured within 100 msec following the initiation of the voltage pulse. Current amplitudes for I_C were measured at 900 msec and for I_D at 1600 msec. Note that a component of I_C can be observed superimposed on the transient component of the I_A current in the most depolarized range

voltage range (−60 to 0 mV), (*iii*) recovery from inactivation was more rapid for I_B, with little cumulative inactivation during repetitive pulses, and (*iv*) I_B could be characterized by the presence of incomplete inactivation during maintained depolarization, accounting for the observed lack of cumulative inactivation (the threshold for current inactivation was +30 mV) and finally, (*v*) I_B was inhibited at low external TEA concentrations (4 mM).

Characterization of I_B current was carried out, in general, in the presence of Ba^{2+} (40 μM) to block inward rectifier current, Zn^{2+} (4 μM) to block the delayed outward current, I_D, and SITS (1 mM) to block the Cl^- current, I_{Cl^-}. Figure 2*A* illustrates control I_B currents taken from a holding potential of −20 mV, a potential at which steady-state inactivation for I_A is complete. The internal K^+ concentration was then changed by internally perfusing the pipette, according to the method of Soejima and Noma (1984), with a solution in which all the K^+ had been replaced with Cs^+ (Fig. 2*B*). The residual currents obtained in the presence of internal Cs^+ which blocked I_B current activation, were then used to leak subtract the current data in Fig. 2*A*. The leak subtracted data were used to construct the peak current-voltage plot in Fig. 2*E*. In order to ascertain the ionic selectivity of I_B, the instantaneous current-voltage relationship was determined from tail current experiments performed in bath solution containing 30 mM K^+ (Fig. 2*C*) and in the presence of bath solution in which all the Na^+ had been isotonically replaced with K^+ (Fig. 2*D*). Instantaneous current reversal potentials were determined by a +80-mV depolarizing prepulse for 40 msec and estimating the potential at which the tail current appeared to reverse polarity during successive repolarizing steps to increasing hyperpolarizing potentials. In experiments similar to that depicted in Fig. 2, the apparent shift in the reversal potential of the instantaneous current-voltage relationship was 24.2 ± 2 mV (n = 7), to be compared to the predicted shift of 40 mV. The current appeared to be predominantly K^+ selective based on the shift in reversal potential in the presence of changes in external K^+, and therefore, a current reversal potential of −82 mV (predicted Nernst potential based on normal internal and external K^+ concentrations) was used to determine the peak conductance *versus*

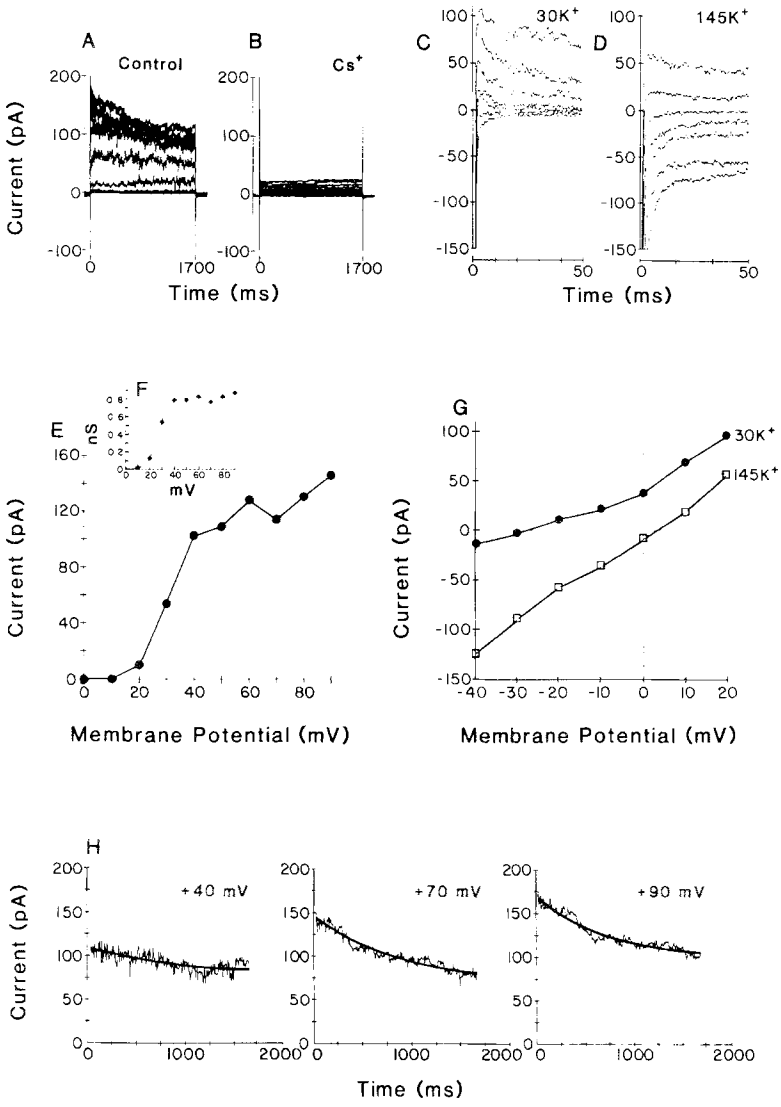

Fig. 2. The kinetics and selectivity of the residual inactivating outward current, I_B (*A*) Control recording of the slowly inactivating outward current in the presence of 4 μM Zn^{2+} to block I_D current and 1 mM SITS to block I_{Cl}. Currents were elicited from the depolarized potential of −20 mM where I_A current, if present would be inactivated. (*B*) Currents from the same cell in which all the K^+ in the pipette solution had been replaced isotonically with Cs^+ using internal pipette perfusion as described in the text. These currents were used to leak subtract the data in *A* and the resultant peak currents are plotted in the current-voltage plot in *E*. (*C*) Tail currents in 30 mM K^+ bathing solution which contained both Zn^{2+} (4 μM), DPC (1 mM), and Ba^{2+} (100 μM) to block contaminating outward and inward currents. Cell was held at −20 mV, stepped to +80 mV for 40 msec, then stepped to the seven increasingly hyperpolarizing potentials used to construct the instantaneous current-voltage plot in *G*. (*D*) Tail currents in 145 mM K^+ bathing solution containing Zn^{2+} and Ba^{2+}. Inspection of the tail currents reveals that the rate of channel deactivation or closure was slowed in the presence of elevated external K^+. (*E*) Current-voltage plot for the leak subtracted currents in *A*. (*F*) Conductance *versus* voltage plot for the currents in *A* using a current reversal potential of −82 mV. (*G*) Instantaneous current-voltage plot for the tail currents in *C* and *D*. (*H*) Theoretical fits to the current data in *A* taken at +40, +70, and +90 mV, respectively. The time constant describing current inactivation was 848 msec at +40 mV, 833 msec at +70 mV, and 676 msec at +90 mV

voltage curve in Fig. 2*F*. The continuous line through the data points in Fig. 2*F* represents the best fit of the peak conductance to a Boltzmann distribution of the form:

$$g(V) = g_{max}/(1 + e^{(V-V_{1/2})/k}) \quad (1)$$

where $V_{1/2}$ is the voltage at the midpoint of the conductance curve and k gives the steepness of the voltage dependence. In three experiments, the $V_{1/2}$ as derived from similar fits to the conductance *versus* voltage curves was 29.7 ± 4.0 mV and k was −8.2 ± 1.7.

The time constant for current inactivation was independent of voltage in the range of +40 to +100 mV. Current inactivation was fitted satisfactorily with a single exponential, suggesting that the kinetics of inactivation can be described as a first order process. The time constant for current inactivation was 951 ± 150 msec (15) at +40 mV, 917 ± 136 msec (15) at +70 mV, and 1121 ± 366 msec (6) at +100 mV.

A comparison of cumulative inactivation during a pulse train for I_A and I_B current can be seen in Fig. 3. During repetitive depolarizations applied at 1 Hz, I_A showed almost complete current inactivation upon the second pulse, with negligible inactivation apparent for I_B.

The absence of steady-state inactivation for I_B at depolarized holding potentials is illustrated in Fig. 4. Peak current amplitude was not significantly changed at the more depolarized holding potential of −20 mV. The time-dependent portion of the outward current at +40 mV, however, was blocked in the presence of 40 μM 4-aminopyridine (4-AP) by 64 ± 8% (9 cells). I_A as well as I_B currents were

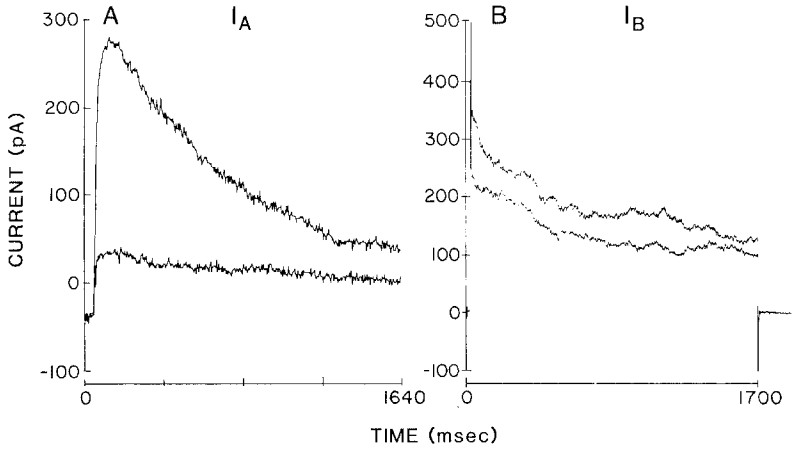

Fig. 3. Inactivation of time-dependent K^+ outward currents. Comparison of the kinetics of inactivation and recovery for I_A and I_B. Whole-cell currents in two cells in response to depolarizing pulses to +80 mV applied at a stimulus frequency of 1 Hz. The holding potential in both cases was −60 mV. Only the first two pulses are shown, the first current being the largest. Note the lack of cumulative inactivation in *B* in response to a pulse train similar to that in *A*

blocked by the classical K^+ channel blocker 4-AP (*see* following paper). Note that I_B as well as the residual time-independent outward current which remains in the presence of 4-AP are inhibited by low concentrations of TEA (Fig. 4*D*). In two cells with prominent I_B expression, I_B current amplitude during depolarizations to +40 mV was reduced by 38 and 40%, respectively, following perfusion of a solution which contained 4 mM Ba^{2+}.

Calcium-Activated K^+ Current (I_C)

The activation of I_C with pipette solutions containing low free-Ca^{2+} levels (38 nM) was characteristically detected as an increase in amplitude in the noise of the current signal at large depolarizations. In experiments where the pipette solution was internally perfused with solutions of increasing Cs^+ concentration, an 88.4 ± 2.5% decrease in I_C amplitude was observed (10 cells). The Cs^+ sensitivity of the currents was determined by replacing the total KCl in the pipette solution with an isosmolar amount of CsCl (Fig. 5*B*). Internal Cs^+ ions have been shown to block Ca^{2+}-activated K^+ channel currents in bovine chromaffin cells (Yellen, 1984) as well as delayed rectifier K^+ currents in peritoneal macrophages (Ypey & Clapham, 1984). A significant (82.0 ± 3.4% (n = 9)) block in current amplitude was also observed when NaCl was used to replace pipette KCl. I_C currents were observed to be time-independent and showed no steady-state inactivation, but could be blocked by the addition of TEA (4 to 10 mM) to the bathing solution (*see* Fig. 4*D*). The outward current at 100 mV was reduced by >52% in four experiments in the presence of external TEA. The exact degree of inhibition was difficult to determine as there appeared to be a second time-independent component of outward current which was TEA insensitive. I_C decreased by 41.1 ± 6.7% (6 cells) in the presence of 4 mM Ba^{2+} in the external solution (*data not shown*). I_C was insensitive to external 4-AP (0.04–4 mM; 19 cells; *see also* Fig. 4*C*).

We did not observe an induction of I_C current expression with time in culture for donors where this conductance was not present at the earliest stages of differentiation. Thus, I_C did not seem to be a marker of differentiation, but rather was expressed at a frequency which varied from donor to donor. This data is to be contrasted with the observations of Gallin and McKinney (1988) which support the conclusion that this conductance is not present in the freshly isolated monocyte but rather is expressed after several days in culture.

Calcium Dependence of Current Activation

I_C appeared similar to the prominent Ca^{2+}-activated K^+ conductance described by Gallin and McKinney (1988) for HMDMs using pipette solutions with a relatively high free-Ca^{2+} (3 μM). Gallin and McKinney (1988) noted that the magnitude of the outward current increased during the first 5 min of recording. They attributed this increase in amplitude to the fact that the pipette free-Ca^{2+} concentration was higher than normal cytoplasmic free-Ca^{2+} levels. For this reason, we investigated I_C current activation in response to changes in internal Ca^{2+} levels. In 9 cells, the internal Ca^{2+} concentration was changed by internally perfusing the pipette with solutions buffered to a higher free-Ca^{2+} concentration. A current record from an internally perfused cell in response to an increase in the internal Ca^{2+} from 38 to 477 nM is illustrated in Fig. 5. An overall increase of 329 ± 125% (n = 5) and 813 ± 212% (n = 5) in current amplitude at 100 mV was associated with an increase in internal Ca^{2+} to 212 and 477 nM, respectively. A shift in the current reversal potential by 22.8 ± 15.8 mV (n = 5) in the hyperpolarizing direc-

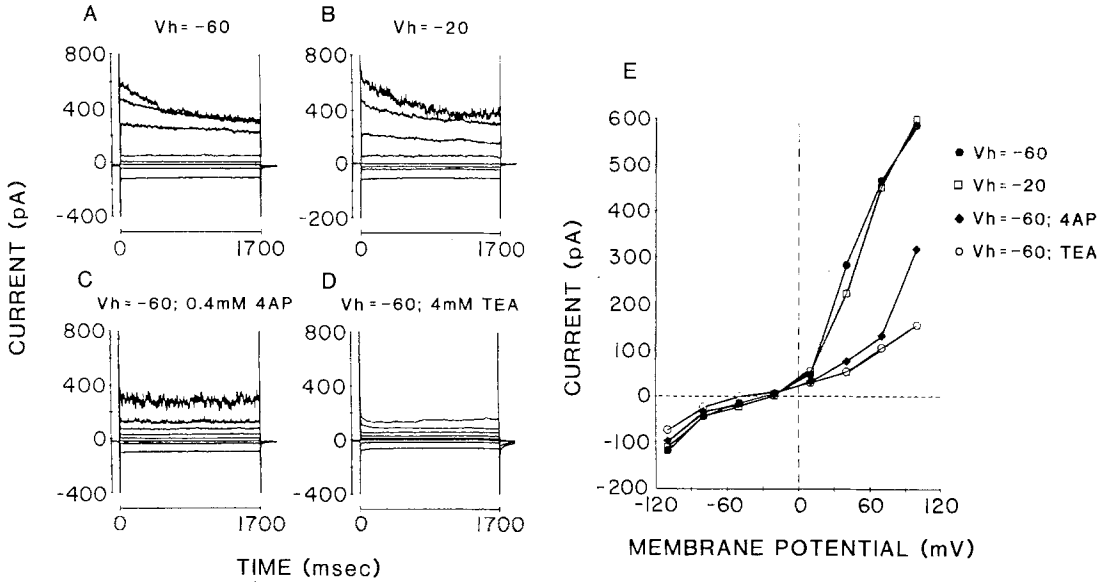

Fig. 4. The absence of steady-state inactivation of I_B at depolarized holding potentials and 4-AP-induced current inhibition. Current records from an adherence isolated 8-day-old cell held at a hyperpolarized (*A*) and depolarized holding potential (*B*). Upon returning to the hyperpolarized holding potential, the bath solution was exchanged for one containing 0.4 mM 4-AP (*C*). Note the block of the time-dependent component of the outward current in the presence of 4-AP leaving a time-independent component of outward current. Following recovery of the time-dependent component from the 4-AP block, the bath solution was exchanged for one containing TEA (4 mM) (*D*), indicating that I_B is also TEA sensitive. (*E*) The associated peak current-voltage relationship

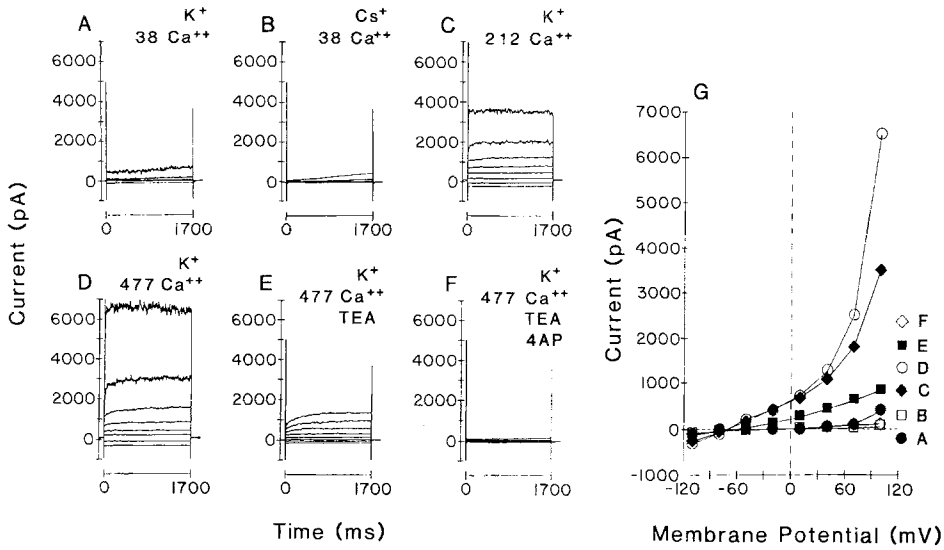

Fig. 5. Activation of Ca^{2+}-dependent whole-cell currents with increasing internal Ca^{2+} concentrations using internal pipette perfusion. (*A*) Whole-cell currents from an adherence isolated, 21-day-old cell in the presence of the standard internal solution buffered to an internal free-Ca^{2+} concentration of 38 nM. (*B*) Current recording from the same cell internally perfused with a pipette solution in which all of the K^+ had been isotonically replaced with Cs^+ and in which the internal free-Ca^{2+} concentration was buffered to 38 nM. Intrapipette solutions were exchanged according to the method of Soejima and Noma (1984). (*C*) Currents in the presence of a standard K^+ pipette solution with the free Ca^{2+} buffered to a concentration of 212 nM. Increasing the internal Ca^{2+} concentration to 212 nM increased the magnitude of both the outward and inward current and, in addition, shifted the current reversal potential in the hyperpolarizing direction by 51 mV. (*D*) A further increase in the amplitude of the outward current was obtained when the pipette was perfused with a solution in which the free-Ca^{2+} concentration was increased to 477 nM. (*E*) Outward current at the elevated internal Ca^{2+} concentration (477 nM) was blocked in the presence of 14 mM external TEA. (*F*) The residual current left after exposure of the cell to TEA was completely inhibited by the addition of 4 mM 4-AP to the TEA containing bath solution. (*G*) The associated current-voltage plot of the data given in *A* through *F*

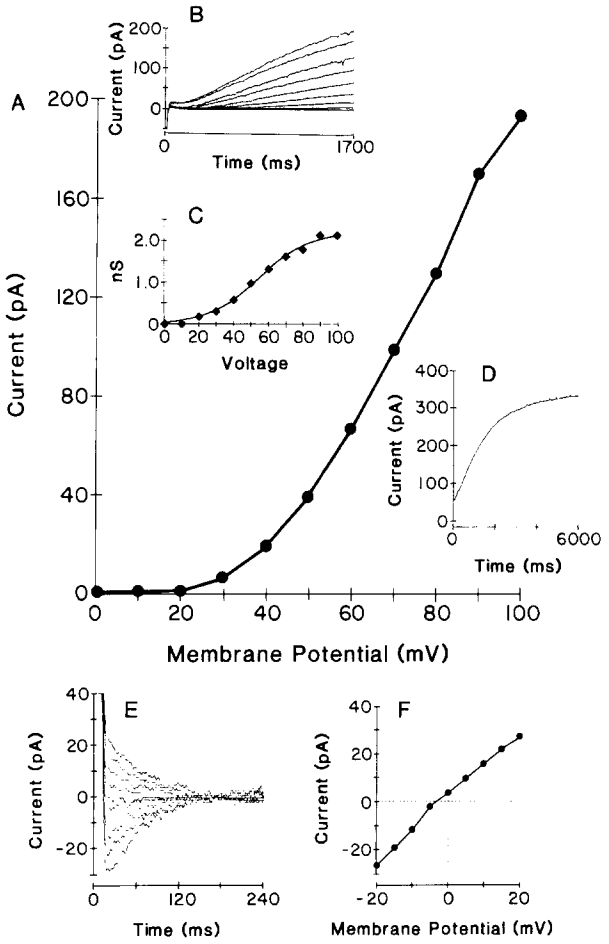

Fig. 6. Kinetics of I_D activation. (*A*) Current-voltage relationship for the whole-cell currents in *B*. (*B*) Whole-cell currents recorded in the presence of internal Cs^+ to block contaminating K^+ currents and 1 mM SITS to block contaminating I_{Cl}. Currents in the presence of 40 μM Zn^{2+} were used to leak subtract the data. (*C*) Associated conductance *versus* voltage plot for the currents in *B* calculated using a current reversal potential of 3.6 mV as determined from tail current experiments. (*D*) Plot of the time dependence of the current at +80 mV. The current reaches steady state at approximately 6 sec. (*E*) Representative tail current experiment and associated current-voltage plot shown in *F*. (*F*) Instantaneous current reversal potential in this experiment was −3.7 mV

tion was associated with an increase in internal Ca^{2+} to 212 nM; a hyperpolarizing shift of similar magnitude (21.3 ± 8.2 mV) (n = 5)) was obtained when internal Ca^{2+} was increased to 477 nM. The current activated as a result of the increase in internal calcium concentration was partially inhibited in the presence of TEA (14 mM, 87% at +100 mV) as seen in Fig. 5*E*. The residual current following exposure to TEA was completely inhibited in the presence of 4-AP (4 mM, Fig. 5*F*).

An increase in the inward as well as outward current with elevated internal Ca^{2+} levels (Fig. 5*C* and *D*) was associated with a hyperpolarizing shift in the reversal potential toward the K^+ equilibrium potential. This suggests that (*i*) I_C is a Ca^{2+}-activated K^+ conductance and (*ii*) there is perhaps more than a single Ca^{2+}-activated conductance pathway. Single-channel data supporting the observation that there may indeed be more than one calcium-activated K^+ conductance has been reported for HMDMs (Randriamampita & Trautmann, 1987; Gallin, 1989) human tonsillar B lymphocytes as well as rat thymocytes (Mahaut-Smith & Schlichter, 1989).

Cation Nonselective Outward Current (I_D)

Following total replacement of the internal K^+ with Cs^+ or Na^+, it was not uncommon to observe a slowly activating component of outward current (I_D) at potentials positive to +20 mV as seen in Fig. 6*B*. During a maintained depolarization to +80 mV the current reached steady state in approximately 6 sec (Fig. 6*D*). The peak current-voltage curve for the currents in Fig. 6*B* is plotted in Fig. 6*A*. I_D activation was inhibited at low external Zn^{2+} (4–400 μM) concentrations. With Cs^+ in the pipette to block contaminating K^+ currents and DPC or SITS in the bath to block chloride current (*vide infra*), a 78 ± 5.4% decrease in outward current was observed at +100 mV in five cells in the presence of Zn^{2+} (40 μM). I_D was the only HMDM current which showed Zn^{2+} sensitivity. Tail current experiments were performed using Cs^+ as a replacement for internal K^+, in the presence and absence of Zn^{2+} (used for leak subtraction). Representative tail currents and associated instantaneous current-voltage plot are depicted in Fig. 6*E* and *F*. The instantaneous current reversal potential of 3.6 ± 4.6 mV (n = 6) as obtained in the tail current experiments was used to construct the conductance *versus* voltage plot in Fig. 6*C*. The smooth line drawn through the peak conductance data points represents the best fit to a Boltzmann distribution in Eq. (1). In two experiments, fits to the data yielded a $V_{1/2}$ of 55.3 and 67 with a slope factor k of −15.5 and −13.2, respectively. The whole-cell chord conductance at the most depolarized potential of +100 mV was 2.3 ± 0.2 nS (n = 21). Tail current reversal potentials were insensitive to Cl^- replacement with either aspartate, glutamate, or gluconate in the external solution indicating that the current was not anion selective.

The cell from which the current recordings in Fig. 7*A* were obtained appeared to express the cation nonselective component of the outward current and a small component of I_C which was blocked by TEA. The selectivity of I_D was further investigated in external anion replacement experiments in the

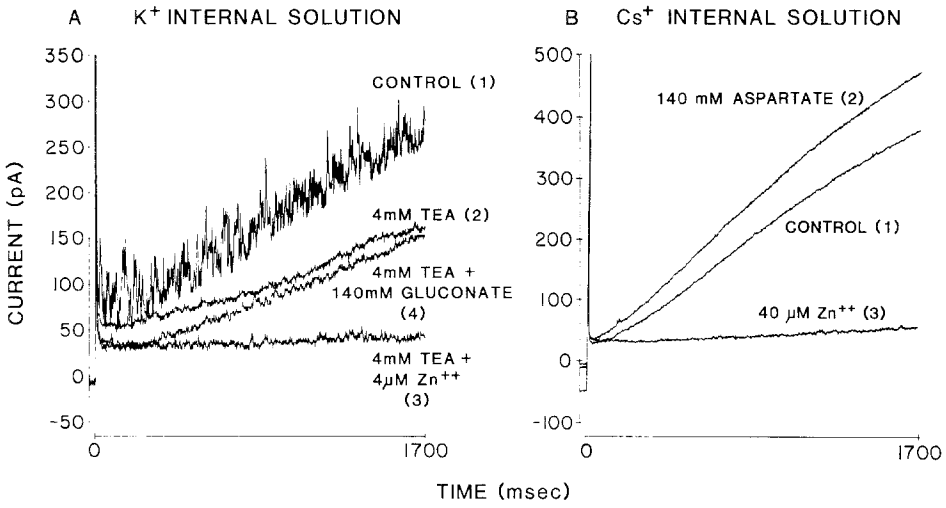

Fig. 7. Zn^{2+} inhibition of I_D. Whole-cell currents recorded from two cells voltage clamped at −60 mV and stepped to +100 mV. (*A*) Intrapipette solution was the standard high K^+ solution. Current records were obtained in the order given by the numbers in parentheses to the right of each current trace. Recordings were made in (*1*) standard Na^+ bathing solution, (*2*) 4 mM TEA bathing solution, (*3*) bathing solution containing 4 mM TEA plus 4 μM Zn^{2+}, and finally, (*4*) in a bathing solution in which all of the Cl^- was replaced with gluconate and in addition contained 4 mM TEA. (*B*) Intrapipette solution K^+ was replaced isosmotically with Cs^+. Current recordings were made in (*1*) normal bath solution, (*3*) bath solution containing 40 μM Zn^{2+}, and (*2*) bath solution in which all of the Cl^- was replaced isosmotically with the impermeant anion aspartate

presence of high internal K^+ (Fig. 7*A*) or high internal Cs^+ (Fig. 7*B*). The substitution of external gluconate or aspartate for Cl^- failed to significantly decrease the magnitude of I_D (Fig. 7*A* and *B*) indicating that the conductance is unlikely to be anion selective, and appears to be cation nonselective in that current was observed in the presence of internal Cs^+, K^+, as well as Na^+ (*see* Figs. 5*B* and 6*B*). In three of the four cells examined, a 39 ± 9% inhibition of I_D was observed in the presence of TEA (4 mM) when contaminating K^+ conductances were blocked by replacement of K^+ with Cs^+ in the internal solution. With Cs^+ as the major cation in the pipette solution, I_D was also inhibited by 51.1 ± 9.3% (n = 3) at low external concentrations of 4-AP (4 mM).

The frequency of I_D current is likely to be underestimated if internal K^+ is not replaced with Cs^+. In many cells, when recorded from under control conditions, only the time-independent I_C current was observed until internal Cs^+ replacements revealed the slowly increasing current at depolarized potentials.

Chloride Current (I_{Cl})

In a large number of cells examined, when Cs^+ or Na^+ was used as an internal K^+ replacement, a time-independent component of outward current remained which was of variable amplitude and which was Zn^{2+}-insensitive. In order to ascertain the ionic species carrying the residual time-independent current, we performed anion substitution experiments. Figure 8 illustrates results obtained when the impermeant anion aspartate was substituted for chloride in the external bathing solution at a ratio of 14 : 1. The reversal potential of the whole cell currents shifted by an average of 36.7 ± 4.0 mV (13) in the presence of aspartate. A shift of 68 mV in the depolarizing direction would have been obtained for a perfectly chloride-selective, aspartate-impermeable membrane. The whole-cell chloride conductances in control conditions (in the absence of aspartate) were 26.8 ± 4.3 nS (n = 6) at +60 mV and 10.6 ± 2.3 nS (n = 6) at −100 mV.

As many anion channels are inhibited by disufonic stilbene derivatives (White & Miller, 1979; Nelson, Tang & Palmer, 1984; Hanrahan, Alles & Lewis, 1985; Valdivia, Dubinsky & Coronado, 1988), we investigated the effects of the irreversible stilbene SITS (1 mM, n = 7) and the reversible stilbene DNDS (200 μM, n = 3). The results of an experiment demonstrating the inhibition of the anion-selective whole-cell current by SITS are presented in Fig. 8*C*. The presence of the stilbene in the bath solution produced a 81.3 ± 5% (n = 7) inhibition of steady-state current amplitude at +100 mV. Similarly, DNDS produced a 59 ± 3.0% inhibition at the same potential (*results not shown*). Significant anion current inhibition was also obtained with the anion channel blockers diphenylamine-2-carboxylate (DPC, 0.2 to 2 mM, 83 ± 2.6%(n = 8)) and anthracene-9-carboxylate (1 mM, 90.5 ± 0.9% (n = 3). Although the chloride channel blockers

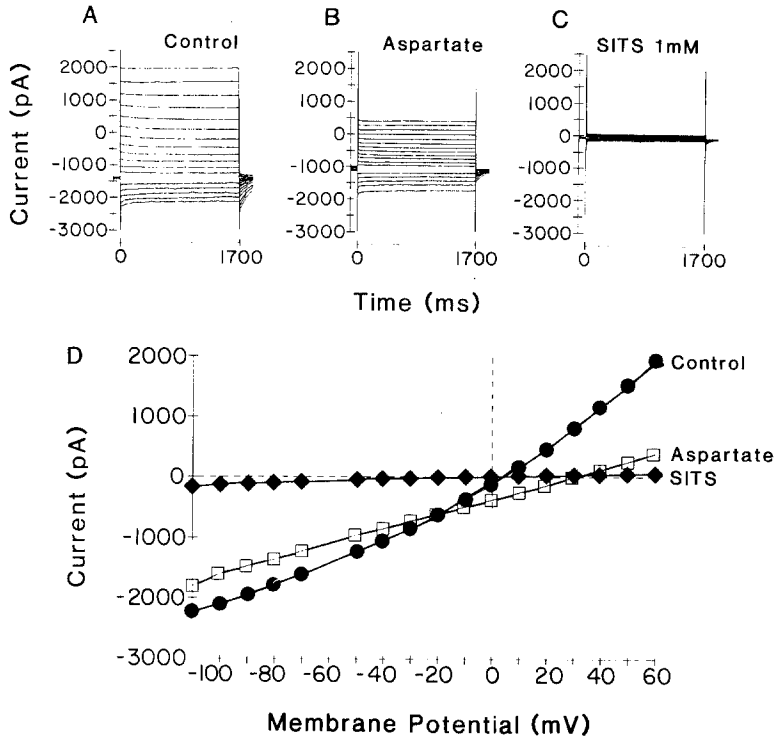

Fig. 8. The selectivity and pharmacology of I_{Cl}. (*A*) Whole-cell currents in the presence of internal Cs^+ to block K^+ currents. Currents were studied over a voltage range in which contamination from I_D was minimal. The internal Ca^{2+} concentration was buffered with EGTA to 38 nM. (*B*) Currents after exchanging the extracellular solution in which most of the external Cl^- had been replaced by aspartate (aspartate to Cl^- ratio was 14:1). (*C*) Currents in the presence of external Cl^- and 1 mM SITS. (*D*) Corresponding current-voltage plot. Control reversal potential was near zero, consistent with the expected 0 mV reversal potential for symmetrical Cl^- solutions. Replacement of most of the Cl^- shifted the reversal potential in the experiment illustrated by 26.1 mV. Current values (at 50 msec) are given for control currents and currents in the presence of aspartate and SITS

DPC and anthracene-9-carboxylate produced a larger reduction of the anion-selective current in the presence of high internal Cs^+ than the stilbene SITS, they, in addition, produced a significant increase in the K^+-selective current in the presence of K^+ pipette solutions containing elevated Ca^{2+} levels as well as an increase in the amplitude of the cation nonselective outward current, I_D. A similar hyperpolarization effect in the presence of anthracene-9-carboxylate has been observed for cells in the thick ascending loop of Henle (Di Stefano et al., 1985).

Inward Rectifier Current

The activation of a prominent time-independent inward current was often observed with increasing hyperpolarization. This current was similar to the inwardly rectifying current described previously by Gallin and Sheehy (1985) for the murine J774 cell and McKinney and Gallin (1988) for the HMDM. As is true of inwardly rectifying K^+ currents previously characterized in a number of excitable tissues (Hagiwara, 1976; Standen & Stanfield, 1978; Hagiwara & Yoshi, 1979; Stanfield, Nakajima & Yamaguchi, 1985), we found that the inwardly rectifying current in HMDMs was detectable at potentials negative to the K^+ equilibrium potential, which in standard bath and pipette solutions was −82 mV. This current increased in amplitude with increasing external K^+ concentration and was blocked by external Ba^{2+} at concentrations as low as 40 μM. A block in inward current at −110 mV of 91.7 ± 1.7% was achieved in the presence of 4 mM Ba^{2+} (10 cells).

Frequency Distribution of Outward Current Types

This investigation included cells obtained from a total of 36 donors, with multiple studies performed on 16 of the donors. Surprisingly, we were unable to relate current expression to state of differentiation, i.e., time in culture, mode of differentiation, or transition from suspension to adherent culture. The occurrence of a given current type appeared to be, however, donor dependent. For a given donor, current frequency patterns were consistent from isolation to isolation, a fact which allowed us to select a given donor for the study of a specific current type. Table 2 gives the frequency of occurrence of each of the four major current patterns for the 974 cells included in the study. A large population of the cells studied exhibited current types which could be described as a combination of the four major types described. Current identification was made on the basis of current (*i*) time dependency, (*ii*) voltage-dependent availability, i.e., the presence of steady-state inactivation, (*iii*) threshold of activation and (*iv*) in some cases, pharmacological sensitivity. As

some cells expressed a combination of currents, exact determination of current frequency was, with the exception of the inactivating I_A current, an underestimate. We did not attempt a frequency distribution estimate of I_{Cl} as that would have entailed a pharmacological dissection of current for all the cells examined. In addition, we did not attempt a rigorous evaluation of the frequency of expression of the inwardly rectifying K^+ current, although it was our impression that it was present at both early and late times in culture differentiation. The distribution of current types from three representative donors are included for comparison in Table 2. Note that donor 1 and donor 3 have an inverse distribution ratio of I_B to I_C. Donor 2 is representative of a class of donors which express I_C at a very low frequency. These distribution ratios remained constant for a given donor throughout time in culture. Of note is the increase in I_A frequency in the Percoll isolated cells. It is possible that I_A current expression in these cells resulted from lymphokine activation due to the fact that the percoll isolated cells were, for the most part, differentiated for variable periods of time in suspension culture before introduction into adherent culture, and the suspension cultures contained from 10–40% lymphocyte contamination.

Table 2. Frequency of whole-cell outward current types in human monocyte-derived macrophages as a function of isolation procedure and donor

	I_A	I_B	I_C	I_D
	Frequency (%)			
HMDM (adherence) (n = 596)	0	66	40	27
Donor 1 (n = 70)	0	81	60	54
Donor 2 (n = 41)	0	93	7	38
Donor 3 (n = 44)	0	71	91	27
HMDM (Percoll) (n = 378)	13	35	66	29

Current identification was made on the basis of current (1) time dependency, (2) threshold of activation, and (3) pharmacological sensitivity in voltage-clamp experiments similar to those depicted in Fig. 1 and expressed as a percentage of the total number of cells for a given donor or experimental isolation technique. As some cells expressed a combination of currents, exact determination of current frequency may in some instances be an underestimate. Current frequencies for a given donor were determined over at least two separate isolations.

Discussion

We observed that HMDMs exhibit a number of voltage- and time-dependent currents with variable expression from donor to donor. Four of these current are carried by K^+. The HMDMs in these studies exhibited two 4-AP-sensitive, time-dependent, outward K^+ currents that could be differentiated by their steady-state inactivation in the physiological potential range, time course of inactivation with maintained depolarization, and threshold of activation. The 4-AP-insensitive component of the outward current activated at potentials positive to +10 mV. One component of the 4-AP-insensitive outward current increased in amplitude as a function of internal Ca^{2+} concentration, could be inhibited in the presence of external TEA, and is undoubtedly the same Ca^{2+}-activated K^+ conductance previously described by Gallin and McKinney (1988) in HMDMs. Following total replacement of the internal K^+ with either Cs^+ or Na^+, a delayed component of outward current remained which had a threshold of activation at approximately +30 mV and could be blocked at low concentrations of external Zn^{2+}. The reversal potential of the delayed outward current, as determined from tail current studies, was approximately 4 mV and insensitive to anion substitution in the external bathing solution, indicating that current was cation nonselective. In the absence of all contaminating K^+ currents, we were able to identify an outwardly rectifying chloride current that could be inhibited by the stilbene SITS. The activation of a prominent time-independent inward current was often observed with increasing hyperpolarization and corresponded to the inwardly rectifying K^+ rectifier current. Table 3 is a summary of the characteristics of the conductances which we have characterized in the HMDM.

Transient Outward Current I_A

The properties of the fast inactivating, transient component of the outward current, I_A, which we observed in HMDMs, suggest its similarity to K^+ currents previously described in human T lymphocytes (Matteson & Deutsch, 1984; Cahalan et al., 1985), in murine clonal cytotoxic T lymphocytes (Fukushima, Hagiwara & Henkart, 1984), in cultured murine macrophages (Ypey & Clapham 1984), in J774.1 and P338D1 cells, murine-derived macrophage-like tumor cells lines (Gallin & Sheehy, 1985; Sheridan & Bayer, 1986), in murine B lymphocytes and their precursors (Choquet et al., 1987), in mammalian platelets (Maruyama, 1987), and in a human cytotoxic T lymphocyte clone (Lee et al., 1986). As has been previously observed for HMDMs (Gallin & McKinney, 1988), this current is the most infrequent of the current types which were observed in the study, in stark contrast to the frequency of expression for this current in the murine peritoneal

Table 3. Summary of whole-cell current characterization in HMDMs

Current type	Time dependency	V_H sensitivity	Threshold voltage	Charge carrier	Blocking agent sensitivity				
					4AP (4 mM)	TEA (4 mM)	Ba^{2+} (4 mM)	Zn^{2+} (4 μM)	DPC SITS
I_A	+++	+++	−40	K^+	+++	ND	ND	ND	—
I_B	+	+	0	K^+	+++	+++	++	—	—
I_C	—	—	+10	K^+	—	+++	++	—	—
I_D	+	—	+30	Nonselective cation	++	++	—	+++	—
I_{IR}	—	—	−85	K^+	—	—	+++	—	—
I_{Cl}	—	—	None	Cl^-	ND	ND	ND	ND	+++

The pharmacology of I_A is incomplete (indicated by the abbreviation ND) due to the low frequency at which the current was observed in our experiments. The symbols +++ indicated in the blocking agent columns correspond to current inhibition of greater than 60%, ++ corresponds to a current inhibition of 30–60%, while + corresponds to current inhibition less than 30%. Current inhibition was determined as the percent decrease in peak current amplitude at +10 mV for I_A, +40 mV for I_B, +100 mV for I_C, +100 mV for I_D, −110 mV for I_{IR}, and +100 mV for I_{Cl}.

macrophage. The difference in the frequency of I_A current observation between the Percoll and adherence purified cells in our studies could be due to the presence of contaminating lymphocytes (10–40%) in the Percoll isolated cells during incubation in suspension. It is likely that the presence of lymphokines could enhance expression of this current which has been related to mitogen stimulation in murine T lymphocytes (DeCoursey et al., 1987*a*).

Calcium-Activated Outward Current I_C

Two prominent voltage-dependent K^+ conductances have been recently characterized in HMDMs at both the whole-cell and single-channel level by Gallin and McKinney (1988): (*i*) a Ca^{2+}-activated K^+ conductance which is TEA and charybdotoxin-sensitive and (*ii*) an inwardly rectifying K^{2+} current which is blocked by external Ba^{2+} and increased with elevation of the external K^{2+} concentration. We have identified and characterized similar currents in the cells described in this study. In our studies, however, the Ca^{2+}-activated K^+ current, I_C, could not be correlated with degree of differentiation as in the studies of Gallin and McKinney (1988) where whole-cell current expression was predicted on the basis of single-channel observations in isolated patch experiments. The discrepancy between our observations on the frequency of I_C expression and those previously obtained for the cultured human cells, as extrapolated from single-channel patch experiments, could result from the fact that at low current densities, during the early stages of differentiation when I_C amplitude is low, patch experiments may fail to sample adequate membrane surface area to predict actual magnitudes of channel expression.

An average increase in the Ca^{2+}-dependent K^+ conductance, using internal solutions with elevated Ca^{2+} concentrations, has been observed for both murine J774 cells and peritoneal macrophages (Randriamampita & Trautmann, 1987). In their studies, Randriamampita and Trautmann, observed that the average input conductance increased ninefold over a range of internal free Ca^{2+} concentrations of 100 nM to 1 μM for the J774 cells. A fivefold increase in conductance was observed for the peritoneal cells over the larger concentration range of 10 nM to 3 μM. In the experiments described in our studies, where each cell served as an internal control, we observed an average eightfold increase in outward current amplitude when the internal free Ca^{2+} was increased from 38 to 477 nM. In the studies of Gallin and McKinney (1988) on HMDMs, the Ca^{2+}-activated K^+ currents, at both the single-channel and the whole-cell level, had similar voltage dependencies. In their experiments, depolarization beyond +30 mV was needed to significantly activate the currents even at the higher internal Ca^{2+} level of 3 μM. Single Ca^{2+}-activated K^+ channel data derived from cell-free patches in the earlier work of Gallin (1984), again using HMDMs, demonstrated the channel open-state probability was 0.5 at +20 mV for a internal Ca^{2+} concentration of 3 μM. Our data, using internal pipette perfusion, shows significant channel activation in the hyperpolarized voltage range (approximately −50 mV) at an internal free-Ca^{2+} concentration of 212 nM. This is to be com-

pared to the threshold of I_C current activation of approximately +10 mV for an internal free Ca^{2+} of 38 nM. Similar shifts in the voltage dependence of current activation at elevated internal Ca^{2+} levels were seen for the murine cells in the studies of Randriamampita and Trautmann (1987).

Previously Uncharacterized Macrophage Currents

We have characterized three additional currents in human macrophages which have, heretofore, not been identified in electrophysiological studies of macrophages: the residual inactivating outward current I_B, the delayed outward current I_D, and the chloride current I_{Cl}.

Residual Inactivating Outward Current I_B

The transient component of the outward current which did not exhibit steady-state inactivation, I_B, bears resemblance to the MRL-1 K^+ currents described in murine T lymphocytes (DeCoursey et al., 1987*b*). Both of these currents inactivate more slowly and less completely during maintained depolarizations possibly accounting for the lack of voltage-dependent current availability. Our inability to demonstrate steady-state inactivation for I_B may also be due to the fact that voltage-dependent availability is observable only in a very depolarized voltage range. Both MRL-1 and I_B currents appear to be sensitive to external TEA; however, we have not made a rigorous comparison between TEA *versus* 4-AP sensitivity in our studies.

We were unable to demonstrate that both transient outward current types coexist in the same cell as had been seen for the MRL-*n* and MRL-1 K^+ currents in the murine T lymphocyte (DeCoursey et al., 1987*b*). The absence of voltage-dependent conductance activation in the hyperpolarized voltage range for cells expressing I_B was in striking contrast to voltage-dependent current activation around −40 mV as was observed in cells expressing I_A. Bimodal conductance *versus* voltage plots with humps around −40 mV were not observed at either hyperpolarized or depolarized holding potentials and would have been expected for cells which predominantly expressed I_B and to a lesser extent I_A.

The shift in the instantaneous current-voltage relationship as a function of increasing external K^+ concentrations was less than the theoretically predicted value indicating that I_B channels may be somewhat less selective for K^+ than I_A channels. Thus, the two types of transient outward current appear to be distinguishable on the basis of selectivity and parameters of activation and inactivation. Three lines of experimental evidence support the conclusion that I_A and I_B represent two separate currents: (*i*) I_B currents activated at potentials approximately 47 mV more positive than I_A currents ($V_{1/2}$ for I_A was −18 mV (*see* Nelson et al. 1990) and $V_{1/2}$ for I_B was 30 mV). (*ii*) In the voltage range of −60 to 0 mV I_B showed no steady-state inactivation; the midpoint for steady-state inactivation for I_A was −44 mV (*see* Nelson et al., 1990). (*iii*) Recovery from inactivation for I_B was practically complete within 1 sec while the time constant describing the recovery from inactivation for I_A was approximately 28 sec (*see* following paper).

Cation Nonselective Outward Current I_D

The delayed outward current I_D which appears in the presence of either K^+, Cs^+, or Na^+ in the pipette solution and is activated in the highly depolarized range is insensitive to isosmotic replacement of external chloride with the impermeant anion substitute gluconate. Unlike, I_B and I_C, the frequency of I_D did not appear to be donor dependent. It was observed at a relatively high frequency in all donors following pharmacological block of all other overlying outward currents. This current has a limited sensitivity to external TEA and 4-AP. The time course of activation for the nonselective cation current I_D resembles that of the delayed rectifier K^+ current in heart (Gintant, Matsurra, Datyner & Cohen, 1985; Matsuura, Tsuguhisa & Imoto, 1987) in that it reaches a plateau over a period of seconds.

The delayed outward current I_D could be distinguished from other HMDM currents on the basis of its Zn^{2+} sensitivity. Zn^{2+} have been shown to decrease the resting chloride conductance of frog skeletal muscle (Stanfield, 1970; Woodbury & Miles, 1973); to block Ca^{2+} channels (Nachshen, 1984; for review *see* Hagiwara & Byerly, 1981), to block Na^+ channels (Hille, Woodhull & Shapiro, 1975; Arhem, 1980; Frelin et al., 1986), and to block NMDA (N-methyl-D-aspartate) receptor responses (Westbrook & Mayer, 1987; Mayer, Vyklicky & Westbrook, 1989). The histamine-rich glycoprotein of serum has been shown to bind with high affinity to several nonferous divalent metals and successfully competes for Zn^{2+} with metal-binding serum proteins like albumin and transferrin in equilibrium dialysis experiments (Morgan, 1981; Burch, Blackburn & Morgan, 1987). The histamine-rich glycoprotein may play a role the transport or homeostasis of metal ions and may act as a source of divalents to the circulating monocyte thereby modulating their electrical excitability.

Chloride Current I_{Cl}

The current-voltage relationship for the chloride current I_{Cl}, showed some rectification in the hyperpolarized range. The degree of rectification was much less than that observed for either the cAMP-activated whole-cell chloride current in the peritoneal mast cell (Matthews, Neher & Penner, 1989), the cAMP-regulated chloride channel present in T and B lymphocytes (Chen, Schulman & Gardner, 1989), or the chloride conductance associated the regulatory volume decrease in T lymphocytes (Cahalan & Lewis, 1988). The anion current in the HMDM was inhibited by a range of chloride channel inhibitors. Similar stilbene sensitivity has been demonstrated for the agonist-activated chloride conductance of mast cells (Matthews et al., 1989). Chloride channel blockers have been shown to effect chemotaxis, lysosomal enzyme release, and superoxide anion generation in human neutrophils (Korchak et al., 1980; Skubitz et al., 1989). Kolb and Ubl (1987) studied the induction of an anion-selective current that may be involved in mediating signal transduction in phagocytic cells. They monitored the indirect activation of large conductance anion channels in cell-attached patches during adsorption of zymosan particles to the membrane of freshly isolated murine peritoneal macrophages. Their data indicates a possible role for the activation of an anion-selective current during zymosan-induced phagocytosis. The zymosan-activated channels are similar in conductance and kinetic properties to the large conductance anionic channel (220 to 400 pS) which Schwarze and Kolb (1984) described earlier in membranes of resting peritoneal macrophages.

The single-channel currents reported in the studies of Schwarze and Kolb (1984) and Kolb and Ubl (1987) differ from the whole-cell currents described in these studies in that they were active only in the voltage range of -30 to $+30$ mV and did not show outward rectification upon membrane hyperpolarization. Therefore, the activation of the large conductance chloride channels could not totally account for the anion current which we observed in the HMDMs.

The selectivity of the whole-cell anion currents in the HMDMs is similar to the selectivity of the cAMP-sensitive currents in the peritoneal mast cell (Matthews et al., 1989) and the tracheal epithelial cell (Schoppa et al., 1989), as well as the Ca^{2+}-dependent currents in the lacrimal gland cell (Evans & Marty, 1986). Replacement of the external chloride by either aspartate or glutamate produced a 35-mV shift in the zero current potential in the peritoneal mast cell and tracheal epithelial cell, and a 46-mV shift in the lacrimal cell. The reversal potential of the chloride currents in the HMDMs shifted by 37 mV for similar external chloride replacements, which is to be compared to the 68 mV shift per decade expected for a perfectly anion-selective membrane. The deviation could be due to the fact that (*i*) the anion conductance is not ideally anion selective, i.e., the Cl^-/Na^+ permeability ratio is low, (*ii*) the conductance is partially permeant to aspartate, i.e., the Cl^-/aspartate permeability ratio is low, or (*iii*) the conductance is not a homogeneous conductance. In reversal potential measurements on the mini-chloride channels which are associated with the regulatory volume decrease and which are ubiqitious among various types of T lymphocytes, replacement of the external Cl^- with aspartate produces a significantly larger shift in the current reversal potential of 50 mV and indicates that in lymphocytes aspartate is 0.12 times as permeant as chloride (Cahalan & Lewis, 1988). In the same set of experiments, Cahalan and Lewis (1988) report that large organic cations, e.g., methansulfonate, used as impermeant anion substitutes, appeared to be significantly permeant.

Summary

In summary, we have examined the variability and frequency of whole-cell currents in HMDMs grown and differentiated in culture. We observed an increase in cell capacitance and a decrease in input resistance which accompanies growth in culture. We characterized three voltage-dependent K^+ selective outward currents: (*i*) an inactivating, 4-AP-sensitive, transient outward current, (*ii*) a 4-AP and TEA-sensitive transient component of the outward current which did not exhibit steady-state inactivation in the physiological potential range and a (*iii*) Ca^{2+}-activated, time-independent component of the outward current which is TEA sensitive. In addition, we identified a delayed outward current which activated in the highly depolarized range, was Zn^{2+} inhibitable, and appeared to be a nonselective cation conductance. Cells also expressed an inward current which resembles the inwardly rectifying K^+ current of nerve and muscle in its Ba^{2+} sensitivity as well as its sensitivity to increases in external K^+ concentration. In the absence of all contaminating K^+, as well as nonselective cation conductances, an outwardly rectifying chloride selective current remained which could be inhibited by the irreversible stilbene SITS. Neither inward nor outward current expression appeared dependent on whether cells were differentiated in adherent or suspension culture nor was demonstrable differential current ex-

pression observed upon transition from suspension to adherent form.

The authors wish to thank Drs. J. Zeller for the Percoll isolated cells used in the initial stages of this investigation, and C. Katnik for critical reading of the manuscript. This work was supported by NIH grant RO 1 GM-36823.

References

Arhem, P. 1980. Effects of some heavy metal ions on the ionic currents of myelinated fibres from *Xenopus laevis*. *J. Physiol. (London)* **306:**219–231

Bennett, W.E., Cohn, Z.A. 1966. The isolation and selected properties of blood monocytes. *J. Exp. Med.* **123:**145–59

Burch, M.K., Blackburn, M.N., Morgan, W.T. 1987. Further characterization of the interaction of histidine-rich glycoprotein with heparin: Evidence for the binding of two molecules of histidine-rich glycoprotein by high molecular weight heparin and for the involvement of histidine residues in heparin binding. *Biochemistry* **26:**7477–7482

Cahalan, M.D., Chandy, K.G., DeCoursey, T.E., Gupta, S. 1985. A voltage-gated potassium channel in human lymphocytes. *J. Physiol. (London)* **358:**197–237

Cahalan, M.D., Lewis, R.S. 1988. Role of potassium and chloride channels in volume regulation by T lymphocytes. *In:* Cell Physiology of Blood. Society of General Physiologists Series. R.B. Gunn and J.C. Parker, editors. Vol. 43, pp. 281–301. Rockefeller University Press, New York

Chen, J.H., Schulman, H., Gardner, P. 1989. A cAMP-regulated chloride channel in lymphocytes that is affected in cystic fibrosis. *Science* **243:**657–660

Choquet, D., Sarthou, P., Primi, D., Cazenave, P.-A., Korn, H. 1987. Cyclic AMP-modulated potassium channels in murine B cells and their precursors. *Science* **235:**1211–1214

DeCoursey, T.E., Chandy, K.G., Gupta, S., Cahalan, M.D. 1987*a*. Mitogen induction of ion channels in murine T lymphocytes. *J. Gen. Physiol.* **89:**405–4200

DeCoursey, T.E., Chandy, K.G., Gupta, S., Cahalan, M.D. 1987*b*. Two types of potassium channels in murine T lymphocytes. *J. Gen. Physiol.* **89:**379–404

Di Stefano, A., Wittner, M., Schlatter, E., Lang, H.J., Englert, H., Greger, R. 1985. Diphenylamine-2-carboxylate, a blocker of the Cl^--conductive pathway in Cl^- transporting epithelia. *Pfluegers Arch.* **405:**S95–S100

Evans, M.G., Marty, A. 1986. Calcium-dependent chloride currents in isolated cells from rat lacrimal glands. *J. Physiol. (London)* **378:**437–460

Frelin, C., Cognard, C., Vigne, P., Lazdunski, M. 1986. Tetrodotoxin-sensitive and tetrodotoxin-resistant Na^+ channels differ in their sensitivity to Cd^{2+} and Zn^{2+}. *Eur. J. Pharmacol.* **122:**245–250

Fukushima, Y., Hagiwara, S., Henkart, M. 1984. Potassium current in clonal cytotoxic lymphocytes from the mouse. *J. Physiol. (London)* **351:**645–656

Gallin, E.K. 1984. Calcium- and voltage-activated potassium channels in human macrophages. *Biophys. J.* **46:**821–825

Gallin, E.K. 1989. Evidence for a Ca-activated inwardly rectifying K channel in human macrophages. *Am. J. Physiol.* **257:**C77–C85

Gallin, E.K., McKinney, L.C. 1988. Patch-clamp studies in human macrophages: Single channel and whole-cell characterization of two K^+ conductances. *J. Membrane Biol.* **103:**55–66

Gallin, E.K., Sheehy, P.A. 1985. Differential expression of inward and outward potassium currents in the macrophage-like cell line J774.1. *J. Physiol. (London)* **369:**475–499

Gallin, E.K., Sheehy, P.A. 1988. Leukocyte ion channels and their functional implications. *In:* Inflammation: Basic Principles and Clinical Correlates. J.I. Gallin, I.M. Goldstein, and R. Snyderman, editors. pp. 651–664. Raven Press, New York

Gintant, G.A., Datyner, N.B., Cohen, I.S. 1985. Gating of delayed rectification in acutely isolated canine cardiac purkinje myocytes. *Biophys. J.* **48:**1059–1064

Hagiwara, S. 1976. Potassium current and the effect of cesium on this current during anomalous rectification of the egg cell membrane of a starfish. *J. Gen. Physiol.* **67:**621–638

Hagiwara, S., Byerly, L. 1981. Calcium channel. *Annu. Rev. Neurosci.* **4:**69–125

Hagiwara, S., Yoshii, M. 1979. Effects of internal potassium and sodium on the anomalous rectification of the starfish egg as examined by internal perfusion. *J. Physiol. (London)* **292:**251–265

Hamill, O.P., Marty, E., Neher E., Sakmann, B., Sigworth, F.J. 1981. Improved patch-clamp techniques for high-resolution current recording from cells and cell-free membrane patches. *Pfluegers Arch.* **391:**85–100

Hanrahan, J.W., Alles, W.P., Lewis, S.A. 1985. Single anion-selective channels in basolateral membrane of a mammalian tight epithelium. *Proc. Natl. Acad. Sci. USA* **82:**7791–7995

Hille, B., Woodhull, A.M., Shapiro, B.I. 1975. Negative surface charge near sodium channels of nerve: Divalent ions, monovalent ions, and pH. *Philos. Trans. R. Soc. London (Biol.)* **270:**301–318

Johnson, W.D., Jr., Mei, B., Cohn, Z.A. 1977. The separation, long-term cultivation, and maturation of the human monocyte. *J. Exp. Med.* **146:**1613–1626

Kolb, H.A., Ubl, J. 1987. Activation of anion channels by zymosan particles in membranes of peritoneal macrophages. *Biochim. Biophys. Acta* **899:**239–246

Korchak, H.M., Eisenstat, B.A., Hoffstein, S.T., Dunham, P.B., Weissman, G. 1980. Anion channel blockers inhibit lysosomal enzyme secretion from human neutrophils without effecting generation of superoxide anion. *Proc. Natl. Acad. Sci. USA* **77:**2721–2725

Lee, S.C., Sabatha, D.E., Deutsch, C., Prystowsky, M.B. 1986. Increased voltage-gated potassium conductance during interleukin 2-stimulated proliferation of a mouse helper T lymphocytes clone. *J. Cell Biol.* **102:**1200–1208

Mahaut-Smith, M.P., Schlichter, J.L. 1989. Ca-dependent K channels in human B lymphocytes and rat thymocytes. *J. Physiol. (London)* **415:**69–83

Maruyama, Y. 1987. A patch-clamp study of mammalian platelets and their voltage-gated potassium current. *J. Physiol. (London)* **391:**467–485

Matsuura, H., Tsuguhisa, E., Imoto, Y. 1987. An analysis of the delayed outward current in single ventricular cells of the guinea-pig. *Pfluegers Arch.* **410:**596–603

Matteson, D.R., Deutsch, C. 1984. K^+ channels in T lymphocytes: A patch clamp study using monoclonal antibody adhesion. *Nature (London)* **307:**468–471

Matthews, G., Neher, E., Penner, R. 1989. Chloride conductance activated by external agonists and internal messengers in rat peritoneal mast cells. *J. Physiol. (London)* **418:**131–144

Mayer, M.L., Vyklicky, L., Jr., Westbrook, G.L. 1989. Modulation of excitatory amino acid receptors by group IIB metal cations in cultured mouse hippocampal neurones. *J. Physiol. (London)* **415:**329–350

McKinney, L.C., Gallin, E.K. 1988. Inwardly rectifying whole-cell and single-channel K currents in the murine macrophage cell line J774.1. *J. Membrane Biol.* **103:**41–53

Morgan, W.T. 1981. Interactions of the histidine-rich glycoprotein of serum with metals. *Biochemistry* **20:**1054–1061

Nachshen, D.A. 1984. Selectivity of the Ca binding site in synaptosome Ca channels. Inhibition of Ca influx by multivalent metal cations. *J. Gen. Physiol.* **83:**941–967

Nelson, D.J., Jow, B., Popovich, K.J. 1990. Whole-cell currents in macrophages: II. Alveolar macrophages. *J. Membrane Biol.* **117:**45–55

Nelson, D.J., Tang, J.M., Palmer, L.G. 1984. Single-channel recordings of apical membrane chloride conductance in A6 epithelial cells. *J. Membrane Biol.* **80:**81–89

Provencher, S.W. 1976. A Fourier method for the analysis of exponential decay curves. *Biophys. J.* **16:**27–41

Randriamampita, C., Trautmann, A. 1987. Ionic channels in murine macrophages. *J. Cell Biol.* **105:**761–769

Schoppa, N., Shorofsky, S.R., Jow, F., Nelson, D.J. 1989. Voltage-gated chloride currents in cultured canine tracheal epithelial cells. *J. Membrane Biol.* **108:**73–90

Schwarze, W., Kolb, H.A. 1984. Voltage-dependent kinetics of an anionic channel of large unit conductance in macrophages and myotube membranes. *Pfluegers Arch.* **402:**281–291

Sheridan, R.E., Bayer, B.M. 1986. Ionic membrane currents induced in macrophages during cytolysis. *Fed. Proc.* **45:**1009*a*

Skubitz, K.M., Vercellotti, G.M., Greenberg, C.S., Eaton, J.W. 1989. Impermeant stilbene disulfonic acids block chemotactic peptide receptor function on human granulocytes. *Inflammation* **13:**31–45

Soejima, M., Noma, A. 1984. Mode of regulation of the ACh-sensitive K-channel by the muscarinic receptor in rabbit atrial cells. *Pfluegers Arch.* **400:**424–431

Standen, N.B., Stanfield, P.R. 1978. A potential and time-dependent blockade of inward rectification in frog skeletal muscle fibres by barium and strontium. *J. Physiol. (London)* **280:**1698–191

Stanfield, P.R. 1970. The differential effects of tetraethylammonium and zinc ions on the resting conductance of frog skeletal muscle. *J. Physiol. (London)* **209:**231–256

Stanfield, P.R., Nakajima, Y., Yamaguchi, K. 1985. Substance-P raises neuronal membrane excitability by reducing inward rectification. *Nature (London)* **315:**498–501

Valdivia, H.H., Dubinsky, W.P., Coronado, R. 1988. Reconstitution and phosphorylation of chloride channels from airway epithelium membranes. *Science* **242:**1441–1444

van Furth, R., van der Meer, J.W.M., van Oud Alblas, A.B., Sluiter, W. 1982. Development of mononuclear phagocytes. *In:* Self-Defense Mechanisms: Role of Macrophages. D. Mizuno, Z.A. Cohn, K. Takeya, and N. Ishida, editors. pp. 25–43. Elsevier

Westbrook, G.L., Mayer, M.L. 1987. Micromolar concentrations of Zn^{2+} antagonize NMDA and GABA responses of hippocampal neurons. *Nature (London)* **328:**640–643

White, M.M., Miller, C. 1979. A voltage-gated anion channel from the electric organ of *Torpedo californica*. *J. Biol. Chem.* **254:**10161–10166

Woodbury, J.W., Miles, P.R. 1973. Anion conductance of frog muscle membranes: One channel, two kinds of pH dependence. *J. Gen. Physiol.* **62:**324–353

Wright, S.D., Silverstein, S.C. 1982. Tumor-promoting phorbol esters stimulate C3b and C3b′ receptor-mediated phagocytosis in cultured human monocytes. *J. Exp. Med.* **156:**1149–1164

Yellen, G. 1984. Ionic permeation and blockade in Ca^{+2}-activated K^+ channels of bovine chromaffin cells. *J. Gen. Physiol.* **84:**157–186

Ypey, D.L., Clapham, D.E. 1984. Development of a delayed outward-rectifying K^+ conductance in cultured mouse peritoneal macrophages. *Proc. Natl. Acad. Sci. USA* **81:**3083–3087

Zeller, J.M., Landay, A.L., Lint, T.F., Gewurz, H. 1986. Enhancement of human peripheral blood monocyte respiratory burst activity by aggregated c-reactive protein. *J. Leukocyte Biol.* **40:**769–783

Zuckerman, S.H., Ackerman, S.K., Douglas, S.D. 1979. Long-term human peripheral blood monocyte cultures: Establishment, metabolisms and morphology of primary human monocyte-macrophage cell cultures. *Immunology* **38:**401–411

Received 14 September 1989; revised 5 February 1990